Surface impedance model for extraordinary transmission in 1D metallic and dielectric screens

V. Delgado* **and R. Marqués**

Department of Electronics and Electromagnetism. University of Seville, Avenida de Reina Mercedes, 41012, Seville, Spain

*vdelgado@us.es

Abstract: Extraordinary Optical Transmission of TM waves impinging at oblique incidence on metallic or high permittivity dielectric screens with a periodic distribution of 1D slits or any other kind of 1D defects is analyzed. Generalized waveguide theory altogether with the surface impedance concept are used for modeling such phenomena. A numerical analysis based on the mode matching technique proves to be an efficient tool for the characterization of these structures for any angle of incidence and slit or defect apertures.

OCIS codes: (050.0050) Diffraction and gratings; (050.1960) Diffraction theory.

References and links

1. T. W. Ebbesen, H. J. Lezec, H. F. Ghaemi, T. Thio, and P. A. Wolff, "Extraordinary optical transmission through sub-wavelength hole arrays," Nature (London) **391,** 667–669 (1998).
2. E. Devaux, T. W. Ebbesen, J.-C. Weeber, and A. Dereux, "Launching and decoupling surface plasmons via micro-gratings," Appl. Phys. Lett. **83,** 4936 (2003).
3. A. A. Yanik, M. Huang, O. Kamohara, A. Artar, T. W. Geisbert, J. H. Connor, and H. Altug, "An optofluidic nanoplasmonic biosensor for direct detection of live viruses from biological media," Nano Lett. **10,** 4962–4969 (2010).
4. H. F. Ghaemi, T. Thio, D. E. Grupp, T. W. Ebbesen, and H. J. Lezec, "Surface plasmons enhance optical transmission through subwavelength holes," Phys. Rev. B **58**(15), 6779–6782 (1998).
5. M. Beruete, M. Sorolla, I. Campillo, J. S. Dolado, L. Martín-Moreno, J. Bravo-Abad, and F. J. García-Vidal, "Enhanced millimeter-wave transmission through subwavelength hole arrays," Opt. Lett. **29**(21), 2500–2502 (2004).
6. M. Sarrazin and J. P. Vigneron, "Optical properties of tungsten thin films perforated with a bidimensional array of subwavelength holes," Phys. Rev. E **68,** 016603 (2003).
7. J. B. Pendry, L. Martín-Moreno, and F. J. García-Vidal, "Mimicking surface plasmons with structured surfaces," Science **305,** 847–848 (2004).
8. R. Marqués, F. Mesa, L. Jelinek, and F. Medina, "Analytical theory of extraordinary transmission through metallic diffraction screens perforated by small holes," Opt. Express **17**(7), 5571–5579 (2009).
9. V. Delgado, R. Marqués, and L. Jelinek, "Analytical theory of extraordinary optical transmission through realistic metallic screens," Opt. Express **18**(7), 6506–6515 (2010).
10. V. Delgado, R. Marqués, and L. Jelinek, "Extraordinary transmission through dielectric screens with 1D subwavelength metallic inclusions," Opt. Express **19**(14), 13612–13617 (2011).
11. J. D. Jackson, *Classical Electrodynamics,* 3rd Ed. (John Wiley & Sons, Inc., 1998)
12. J. A. Porto, F. J. Garcia-Vidal, and J. B. Pendry, "Transmission resonances on metallic gratings with very narrow slits," Phys. Rev. Lett. **83,** 2845–2848 (1999).
13. F. J. García-Vidal and L. Martín Moreno, "Transmission and focusing of light in one-dimensional periodically nanostructured metals," Phys. Rev. B **66,** 155412 (2002).
14. M. M. J. Treacy, "Dynamical diffraction explanation of the anomalous transmission of light through metallic gratings," Phys. Rev. B **66,** 195105 (2002).

#151740 - $15.00 USD Received 28 Jul 2011; revised 23 Sep 2011; accepted 20 Oct 2011; published 23 Nov 2011

15. F. Medina, F. Mesa, D. C. Skigin, "Extraordinary transmission through arrays of slits: a circuit theory model," IEEE Trans. Microwave Theory Tech. **58**(1), 105–115 (2010).
16. M. A. Ordal, L. L. Long, R. J. Bell, S. E. Bell, R. R. Bell, R. W. Alexander,Jr., and C. A. Ward, "Optical properties of the metals Al, Co, Cu, Au, Fe, Pb, Ni, Pd, Pt, Ag, Ti, and W in the infrared and far infrared," Appl. Opt. **22**(7), 1099–1119 (1983).
17. P. H. Bolivar, J. G. Rivas, R. Gonzalo, I. Ederra, A. L. Reynolds, M. Holker, and P. de Maagt, "Measurement of the dielectric constant and loss tangent of high dielectric-constant materials at terahertz frequencies," IEEE Trans. Microwave Theory Tech. **51**(4), 1062–1066 (2003).

1. Introduction

The phenomenon of Extraordinary Optical Transmission (EOT) through opaque screens with a periodic array of subwavelength holes, first reported in [1], is a current topic of intensive research due to its potential applications in photonic circuits [2], optical sensing [3] or fabrication of left-handed metamaterials. As nanofabrication techniques improve, efficient numerical models are desirable in order to provide fast characterization of the designs as well as physical insight into the phenomena. The physical background of the phenomena is an issue of controversy. Channeling of surface plasmons (SP) [4] through the holes was first proposed, but could not explain Extraordinary Transmission (ET) in metals at microwave frequencies [5] or in dielectric screens [6] where real part of permittivity is positive and SP do not exist. Subsequently, the surface plasmon concept was rescued to explain ET after considering that plasmon-like surface waves, or *spoof plasmons*, can be supported by structured metallic or dielectric surfaces [7]. Recently, some of the authors presented an analytical theory of EOT through perfect conducting screens based on waveguide analysis [8]. In this paper the role of *spoof plasmons* in extraordinary transmission was also discussed (see e.g. Table 1 in [8]). This theory was later extended to screens made of realistic conductors such as metals at optical frequencies [9] and 1D dielectric configurations [10]. These generalizations were based on the surface impedance concept, which is widely used in classical electromagnetism for the analysis of skin effect in imperfect conductors [11]. The model in [9, 10] has some limitations as it is only valid in the case of normal incidence and for holes smaller than a quarter wavelength. In this letter, we present a unified analysis of extraordinary transmission at oblique incidence through periodic metallic or dielectric screens, loaded with transparent or opaque defects, including thin (sub-skin-depth) screens and wide ($\sim \lambda/2$) slits or defects.

2. Theory

We will consider a metallic or high permittivity dielectric screen with a periodic distribution of slits. These configurations have been analyzed by many authors [12-15] in order to simplify numerical problems and subsequently have taken on a live of its own. In this section such structure will be analyzed using an approximate mode-matching analysis which is simplified making use of the surface impedance concept.

The unit cell of the structure is depicted in Fig. 1. For an incident TM wave with the magnetic field parallel to the slits and the wave vector in the yz plane, we have a bidimensional problem with no x dependence. The impinging wave imposes phase shift boundary conditions at $y = \pm a/2$. The transverse components of the fields in regions 1, 2 and 3 can be expanded in terms of Bloch and waveguide modes and evaluated in the input and output surfaces of the screen

$$E_y^{(1)}(z=-t/2) = (1+R)\exp[ik_{y,0}y] + \sum_{\substack{n=-N \\ n\neq 0}}^{N} R_n \exp\left[i\left(k_{y,0}+\frac{2n\pi}{a}\right)y\right], \qquad (1)$$

#151740 - $15.00 USD Received 28 Jul 2011; revised 23 Sep 2011; accepted 20 Oct 2011; published 23 Nov 2011

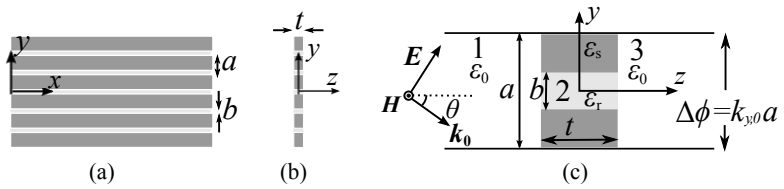

Fig. 1. Front (a) and side (b) view of the screen with a periodic distribution of slits. Unit cell of the structure (c) with the incident TM wave. The impinging wave imposes periodic boundary conditions with a constant phase shift $\Delta\phi = k_{y,0}a$ along y.

$$E_y^{(2)}(z=-t/2) = S_0^+ + S_0^- \exp\left[ik_{z,0}^{(\mathrm{w})}t\right] + \sum_{m=1}^{M}\left(S_m^+ + S_m^- \exp\left[ik_{z,m}^{(\mathrm{w})}t\right]\right)\cos\left(\frac{m\pi}{b}(y+b/2)\right), \tag{2}$$

$$E_y^{(2)}(z=t/2) = S_0^+ \exp\left[ik_{z,0}^{(\mathrm{w})}t\right] + S_0^- + \sum_{m=1}^{M}\left(S_m^+ \exp\left[ik_{z,m}^{(\mathrm{w})}t\right] + S_m^-\right)\cos\left(\frac{m\pi}{b}(y+b/2)\right), \tag{3}$$

$$E_y^{(3)}(z=t/2) = T\exp\left[ik_{y,0}y\right] + \sum_{\substack{n=-N\\ n\neq 0}}^{N} T_n \exp\left[i\left(k_{y,0}+\frac{2n\pi}{a}\right)y\right], \tag{4}$$

where T and R are the transmission and reflection coefficients; T_n, R_n, $S_0^{\pm}$ and $S_m^{\pm}$ are the amplitudes of the different modes excited in the screen; $k_{y,0}$ is the transversal component of the wave vector of the incident wave and

$$k_{z,m}^{(\mathrm{w})} = \sqrt{\varepsilon_{\mathrm{r}}k_0^2 - \left(\frac{m\pi}{b}\right)^2} \tag{5}$$

are the propagation constants of the modes inside the slits which may be filled with a dielectric of relative permittivity ε_{r}. Expressions for magnetic fields $H_x^{(i)}$ are obtained by just multiplying each mode in Eqs. (1)–(4) by its corresponding wave admittance. Expansions in Eqs. (2) and (3) correspond to a parallel plate waveguide with PEC plates at $y = \pm b/2$, so losses or effects of field penetration inside the screen in the inner walls of the slits are neglected. This approximation is plausible only in the case of $\varepsilon_{\mathrm{r}} << \varepsilon_{\mathrm{s}}$, which is also the meaningful case for EOT. A mode-matching analysis is employed to calculate all the coefficients in Eqs. (1)–(4). In this mode-matching analysis, specific relations between the electromagnetic fields at both sides of the screen ($z = \pm t/2$) will be considered. In the area of the slits, continuity of transverse electromagnetic fields is imposed

$$\left.\begin{array}{l} E_y^{(1)}(z=-t/2) = E_y^{(2)}(z=-t/2) \\ E_y^{(2)}(z=t/2) = E_y^{(3)}(z=t/2) \\ H_x^{(1)}(z=-t/2) = H_x^{(2)}(z=-t/2) \\ H_x^{(2)}(z=t/2) = H_x^{(3)}(z=t/2) \end{array}\right\} \text{ for } |y| \le b/2, \tag{6}$$

whereas in the area of the screen, each mode of the transverse electromagnetic fields in regions 1 and 3 evaluated in $z = \pm t/2$ are related through a surface impedance matrix [9]

$$\begin{bmatrix} E_{y,n}^{(3)} + E_{y,n}^{(1)} \\ E_{y,n}^{(3)} - E_{y,n}^{(1)} \end{bmatrix} \approx \begin{bmatrix} Z_n^{(1)} & 0 \\ 0 & Z_n^{(2)} \end{bmatrix} \begin{bmatrix} H_{x,n}^{(3)} - H_{x,n}^{(1)} \\ H_{x,n}^{(3)} + H_{x,n}^{(1)} \end{bmatrix} \text{ for } b/2 \le |y| \le a/2, \tag{7}$$

#151740 - $15.00 USD Received 28 Jul 2011; revised 23 Sep 2011; accepted 20 Oct 2011; published 23 Nov 2011

where

$$Z_n^{(1)} = \frac{\left[1+\cos(k_{z,n}^{(s)}t)\right]}{\mathrm{i}\sin(k_{z,n}^{(s)}t)Y_{s,n}} \text{ and } Z_n^{(2)} = \frac{\mathrm{i}\sin(k_{z,n}^{(s)}t)}{\left[1+\cos(k_{z,n}^{(s)}t)\right]Y_{s,n}}, \tag{8}$$

are the surface impedances corresponding to each mode,

$$k_{z,n}^{(s)} = \sqrt{\varepsilon_s k_0^2 - \left(\frac{2n\pi}{a}\right)^2} \text{ and } \mathrm{Y_{s,n}} = \frac{\omega\varepsilon_s\varepsilon_0}{\mathrm{k_{z,n}^{(s)}}} \tag{9}$$

are the propagation constants and wave admittances of the modes inside the metallic or high permittivity screen and ε_s is the relative permittivity of the screen. The effect of the surface impedance in Eq. (8) is to provide an additional coupling between both sides of the screen, which may be dominant for thin sub skin-depth metallic screens, or in dielectric screens (see discussion in Sec. 3, at the end). It also accounts for losses in the screen.

Matrix equation Eq. (7) is exact in the case of an infinite and homogenous plain slab; however, despite the presence of the slits, it proves to be a powerful approximation and allows us to considerably simplify the mode matching algorithm that strictly should also account for modal expansion inside the screen. When slits are very thin ($t \approx a/100$) the model is less accurate as edge effects become more relevant. In any case, 1D configurations do not yield relevant transmission peaks when the screens are so thin.

Now, multiplying Eq. (6) by

$$\cos\left[\frac{m\pi}{b}(y+b/2)\right],\ m=1,.....,M; \tag{10}$$

and Eq. (7) by

$$\exp\left[-i\left(k_{y,0}+\frac{2n\pi}{a}\right)y\right],\ n=-N,...,0...,N; \tag{11}$$

and integrating in the corresponding ranges of y, we obtain a set of overdetermined equations which can be numerically solved using a least square algorithm.

3. Results

In Figs. 2–6 the transmission coefficients obtained with the reported model are compared with electromagnetic simulations using *CST Microwave Studio*. In order to obtain convergent results, the resolution of the higher modes inside the slits (M) and in the input and output regions (N) must be similar. Convergent results were obtained employing $N = 60$ modes in Eq. (6) and $M \approx N(b/a)$ modes in Eq. (7) with a CPU time of ~ 0.5s vs CPU time of ~ 10s with the electromagnetic solver.

In Figs. 2 and 3 the metallic screen is modeled by a finite conductivity $\sigma = 59.6\times10^6$ S/m (corresponding to copper) at frequencies around 1 THz:

$$\varepsilon_s \approx i\frac{\sigma}{\omega\varepsilon_0}, \tag{12}$$

and in Fig. 4 by a Drude-Lorentz permittivity for silver [16] at frequencies around 300 THz

$$\varepsilon_s \approx \varepsilon_0\left(1-\frac{\omega_p^2}{\omega(\omega-if_c')}\right), \tag{13}$$

#151740 - $15.00 USD Received 28 Jul 2011; revised 23 Sep 2011; accepted 20 Oct 2011; published 23 Nov 2011

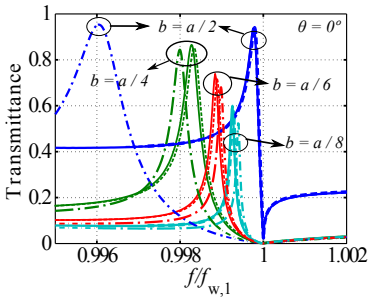

Fig. 2. Transmission through an array of slits in a lossy copper screen ($\sigma = 59.6 \times 10^6 S/m$) at normal incidence and different sizes of the slits. Periodicity is $a = 300\mu$m and thickness of the screen is $t = a/20$. Continuous lines correspond to mode matching model, dashed lines to CST simulations and dot-dashed lines to our previous numerical model [9].

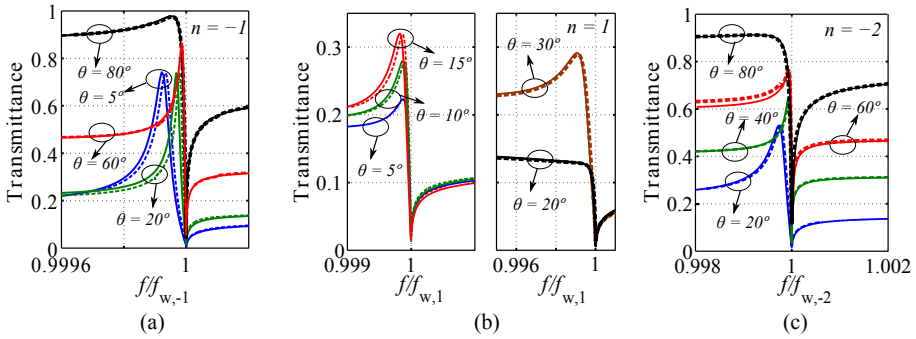

Fig. 3. Transmission through an array of slits in a lossy copper screen ($\sigma = 59.6 \times 10^6 S/m$) for different angles of incidence and Wood's anomalies resonances. Periodicity is $a = 300\mu$m, size of slits is $b = a/4$ and thickness of the screen is $t = a/20$. Continuous lines correspond to mode matching model and dashed lines to CST simulations.

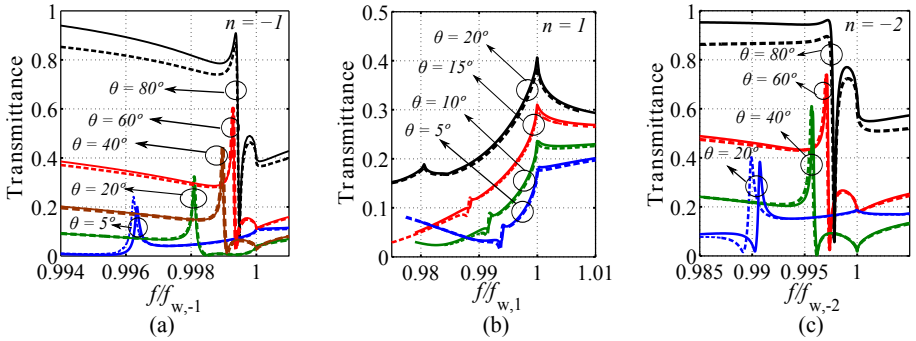

Fig. 4. Transmission through an array of slits in a silver screen ($\omega_p = 2\pi \times 2175THz$ and $f_c' = 1.26 \times f_c = 1.26 \times 2\pi \times 4.35$ THz) for different angles of incidence and Wood's anomalies resonances. Periodicity is $a = 1\mu$m, size of slits is $b = a/4$ and thickness of the screen is $t = a/20$. Continuous lines correspond to mode matching model and dashed lines to CST simulations.

#151740 - $15.00 USD Received 28 Jul 2011; revised 23 Sep 2011; accepted 20 Oct 2011; published 23 Nov 2011

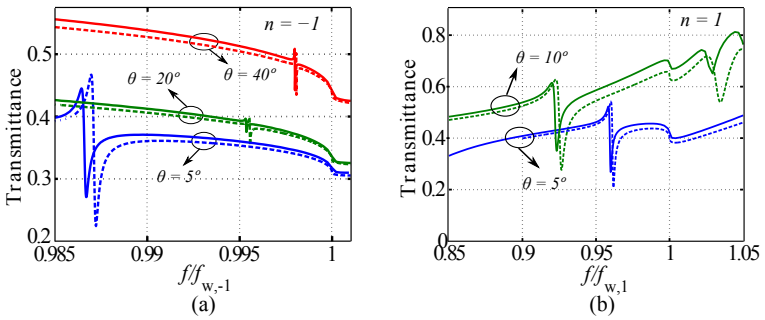

Fig. 5. Transmission through an array of slits in a zirconium-tin-titanate ($\varepsilon = 92.7(1 + 0.005i)$ [17]) screen for different angles of incidence and Wood's anomalies resonances. Periodicity is $a = 3$mm, size of slits is $b = a/6$ and thickness of the screen is $t = a/25$. Continuous lines correspond to mode matching model and dashed lines to CST simulations.

with plasma frequency $\omega_p = 2\pi \times 2175$ THz and frequency of collision $f_c' = 1.26 \times f_c = 1.26 \times 2\pi \times 4.35$ THz, where a correction due to finite thickness of the screen has been taken into account [9]. In the abscissas, frequencies are normalized to the Wood's anomalies frequencies for each angle of incidence

$$f_{w,n} = \begin{cases} \dfrac{nc}{a(1-\sin(\theta))} & \text{for } n > 0 \\ \dfrac{|n|c}{a(1+\sin(\theta))} & \text{for } n < 0 \end{cases} \tag{14}$$

corresponding to the divergence of the TM_{2n} modes excited in the generalized waveguide. In the case of metallic screens, the numerical model works quite well for any angle of incidence and different Wood's anomalies resonances ($n = -1$, $n = 1$ and $n = -2$). At a given angle of incidence ($\theta = 19.47^o$) the Wood's anomaly frequency corresponding to the divergence of the scattered TM_2 and TM_{-4} modes is the same. For higher angles of incidence the peaks corresponding to the divergence of TM_2 mode vanish (Fig. 2(b)) and those corresponding to the divergence of TM_{-4} grow.

In Fig. 2 the numerical model presented here is compared with the model reported in [9]. It can be seen how this previous numerical model, in which variations of orthogonal functions in the region of the small slits are neglected, fails to characterize screens with wide slits. The proposed numerical model also applies to screens made of high permittivity dielectric (Figs. 5 and 6). However, in this case there are some limitations. When the Wood's anomaly frequency is close to a Fabry-Perot resonance and background transmission is close to unity, the numerical model does not provide physically meaningful results. In any case, when background transmission is high, EOT peaks lack practical interest. In Fig. 5 the slits are empty and in Fig. 6 the slits are filled with a PEC ($Z_n^{(1)} = Z_n^{(2)} = 0$), in which case we find that transmission peaks are higher and background transmission lower than in the case of empty slits. This effect was previously reported in [10] for normal incidence. Here is confirmed for all angles of incidence. In computations not shown here, we have checked the validity of the model for lower values of permittivity ($\varepsilon_s \approx 10$). However, for such low values of the permittivity, background transmission is high and EOT peaks lack interest.

In order to gain physical insight into the phenomenon, the longitudinal real part of the Poynting vector ($\Re(S_z)$) at the frequencies of some of the peaks, computed with the electromagnetic simulator are plotted in Fig. 7 and 8. In Fig. 7 the screens are modeled as lossy copper. The

#151740 - $15.00 USD Received 28 Jul 2011; revised 23 Sep 2011; accepted 20 Oct 2011; published 23 Nov 2011

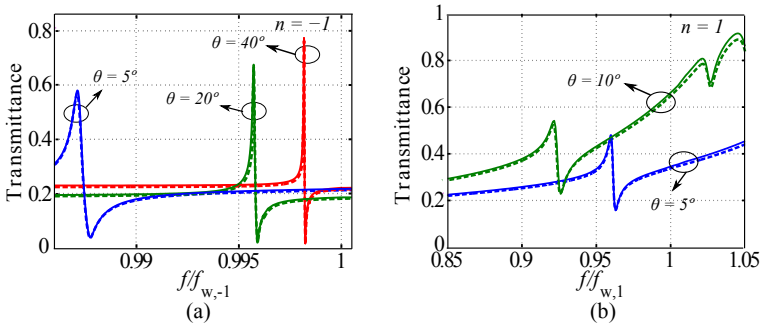

Fig. 6. Transmission through an array of PEC inclusions in a zirconium-tin-titanate ($\varepsilon = 92.7(1+0.005i)$ [17]) screen for different angles of incidence and Wood's anomalies resonances. Periodicity is $a = 3$mm, size of the inclusions is $b = a/6$ and thickness of the screen is $t = a/25$. Continuous lines correspond to mode matching model and dashed lines to CST simulations.

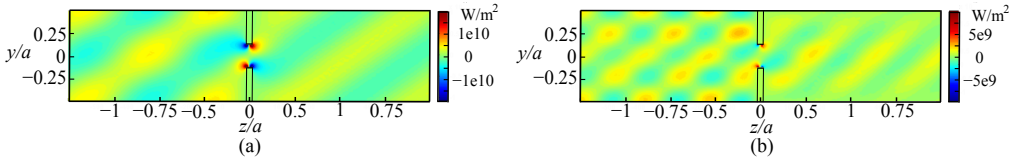

Fig. 7. Propagating component of the real part of the Poynting vector at the frequencies of the EOT peaks for the lossy copper screen analyzed in Fig.2. In (a) EOT is associated to the divergence of the TM_{-2} mode and in (b) to the divergence of the TM_{-4} mode. Angle of incidence is $\theta = 20^o$ in both cases.

graphics are complex, with vortexes of power bouncing forward and backward along the structure; a fact which express the important role played by evanescent modes near the screen. A high concentration of power appears at the edges of the slits, where strong currents are excited. Figure 7(a) corresponds to the divergence of the TM_{-2} mode and Fig. 7(b) to the divergence of the TM_{-4} mode excited in the screen for an angle of incidence $\theta = 20^o$. In both cases, the power flow pattern corresponding to each resonance can be clearly appreciated. In Fig. 8 the screens are modeled as zirconium-tin-titanate ($\varepsilon = 92.7(1+0.005i)$). In Fig. 8(a) the slits are empty and in Fig. 8(b) the slits are filled with PEC. In both cases the patterns correspond to the divergence of the TM_{-2} mode for an angle of incidence $\theta = 20^o$; and show that most power is transmitted through the dielectric screens, thus suggesting that EOT in these structures is obtained as a consequence of the periodic distribution of defects, and no necessarily associated to the presence of transparent slits. Even more, in Fig. 8(a) the empty slits seem to act as a drain of power, which is first transmitted through the dielectric from left to right and then partially put back in the left space through the slits.

4. Conclusion

A new model for oblique incidence EOT in metallic or dielectric screens with 1D periodic arrays of slits or other kind of defects has been provided. The model is based on a combination of the generalized waveguide modal analysis with the surface impedance concept. A numerical technique has been developed based on such model, which allows for the rapid characterization of EOT in metallic or high permittivity dielectric screens loaded with 1D transparent or opaque defects. This technique provides a unified treatment of all these examples, revealing

#151740 - $15.00 USD Received 28 Jul 2011; revised 23 Sep 2011; accepted 20 Oct 2011; published 23 Nov 2011

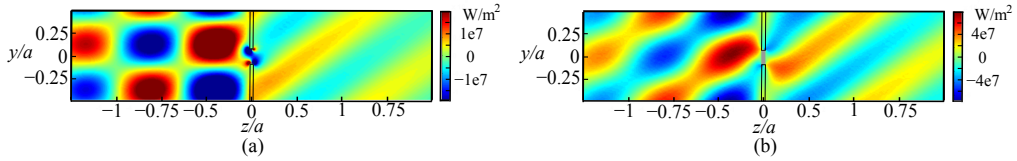

Fig. 8. Propagating component of the real part of the Poynting vector at the frequencies of the EOT peaks for the zirconium-tin-titanate screen analyzed in Figs. 5 and 6. In (a) the slits are empty and in (b) filled with PEC. Angle of incidence is $\theta = 20^o$ and EOT is associated to the divergence of the TM_{-2} mode in both cases.

that the same physics is behind them and that periodicity, instead of the specific mechanism of power transmission, is the relevant physical fact. The analyzed structures could be useful as spatial filters for certain angles of incidence and frequencies. In the case of dielectric screens, metallic inclusions in the slits result in enhanced transmission peaks, suggesting the possibility of interesting phenomena, such as optically induced EOT in photoconductive semiconductor screens.

Acknowledgments

This work has been supported by the Spanish Ministerio de Educación y Ciencia and European Union FEDER funds (project No. CSD2008-00066 and TEC2010-16948). The authors are grateful to Lukas Jelinek for many fruitful discussions.

#151740 - $15.00 USD Received 28 Jul 2011; revised 23 Sep 2011; accepted 20 Oct 2011; published 23 Nov 2011